Progress of Turbulent Transport Studies on Toroidal Plasmas via Gyrokinetic Simulation with GKV

ジャイロ運動論的シミュレーション GKV によるトーラスプラズマ乱流輸送研究の進展

Tomo-Hiko Watanabe
Department of Physics, Nagoya University

In collaboration with
H. Sugama, M. Nunami, A. Ishizawa, S. Toda (NIFS)
Y. Idomura, S. Maeyama, M. Nakata (JAEA)
Y. Asahi (TiTech)

プラズマシミュレータ(核融合科学研究所)、ヘリオス(国際核融合エネルギー研究センター)、京(理化学研究所計算科学研究機構)、の各計算機を利用させていただいた。また、課題の実施においてはHPCI 戦略課題分野4体制構築課題・一般利用課題ならびに科学研究費補助金の支援をいただいた。

Gyrokinetic Simulation Code: GKV

- Nonlinear gyrokinetic equation for perturbed gyrocenter distribution δf is numerically solved on the five-dimensional phase space, $(x, y, z, v_{||}, \mu)$

$$\left[\frac{\partial}{\partial t} + v_{\|}\hat{\mathbf{b}}\cdot\nabla + \mathbf{v}_d\cdot\nabla - \mu\left(\hat{\mathbf{b}}\cdot\nabla\Omega\right)\frac{\partial}{\partial v_{\|}}\right]\delta f + \frac{c}{B_0}\{\psi, \delta f\} = \left(\mathbf{v}_* - \mathbf{v}_d - v_{\|}\hat{\mathbf{b}}\right)\cdot\frac{e\nabla\psi}{T_i}F_M + C(\delta f)$$

  - Strong anisotropy of fluctuations is accurately resolved by using curvilinear coordinates along field lines.
  - High resolution of 5-D phase space.

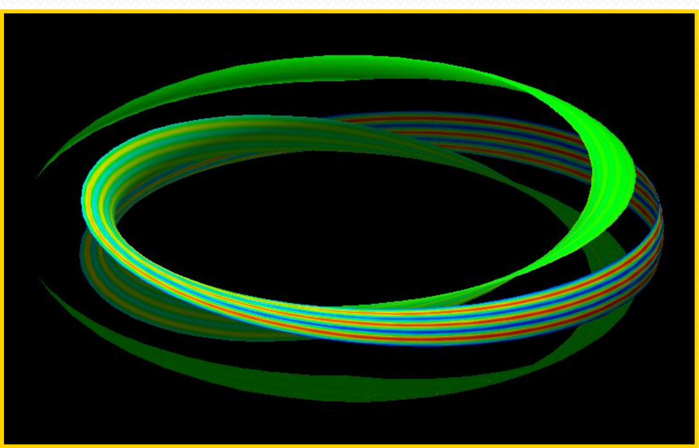

(GKV: Watanabe & Sugama NF 2006)

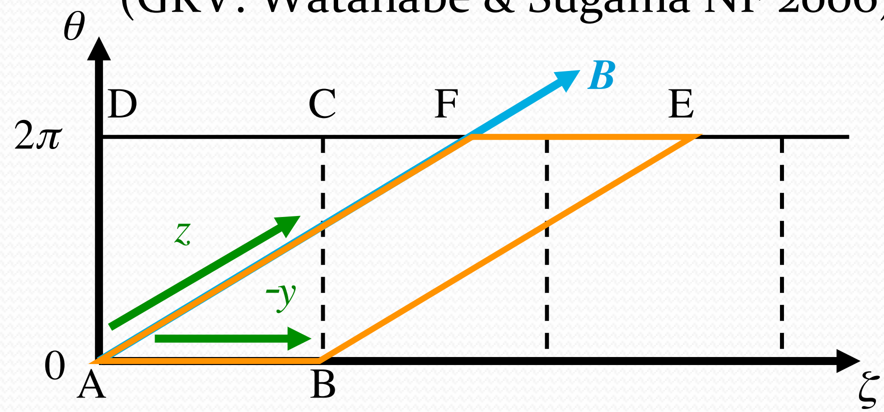

GKV Applications in early days

- Tokamak ITG turbulence and zonal flow
  - Entropy balance relation
  - Zonal flow response function and GAM damping
- Helical ITG turbulence and zonal flow
  - Zonal flow response function influenced by helical field
  - Transport reduction in the inward-shifted LHD plasma

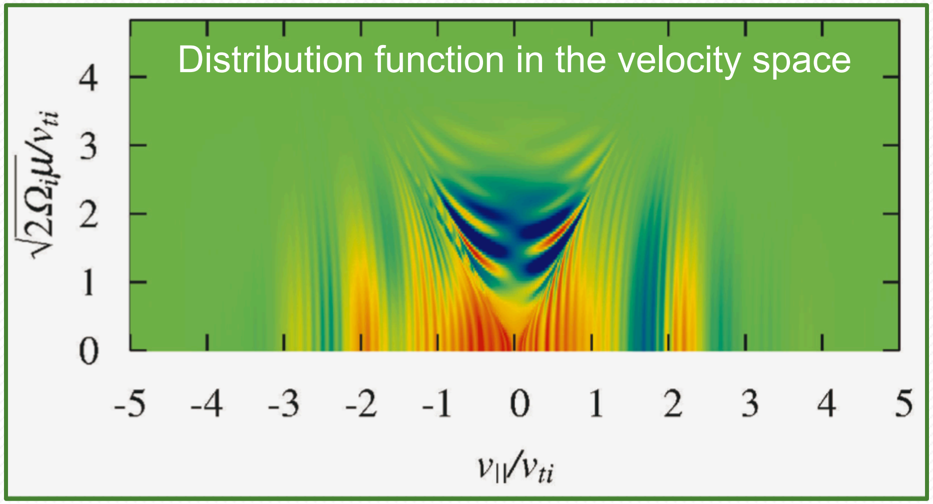

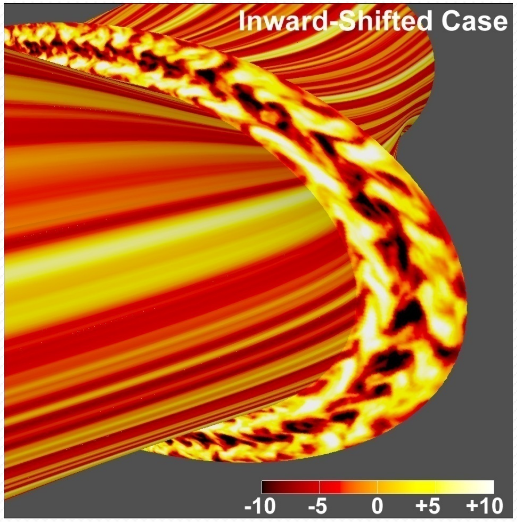

Watanabe, Sugama, Ferrando-Margalet, PRL 2008

Validation of GK simulations against LHD experiments has recently been advanced

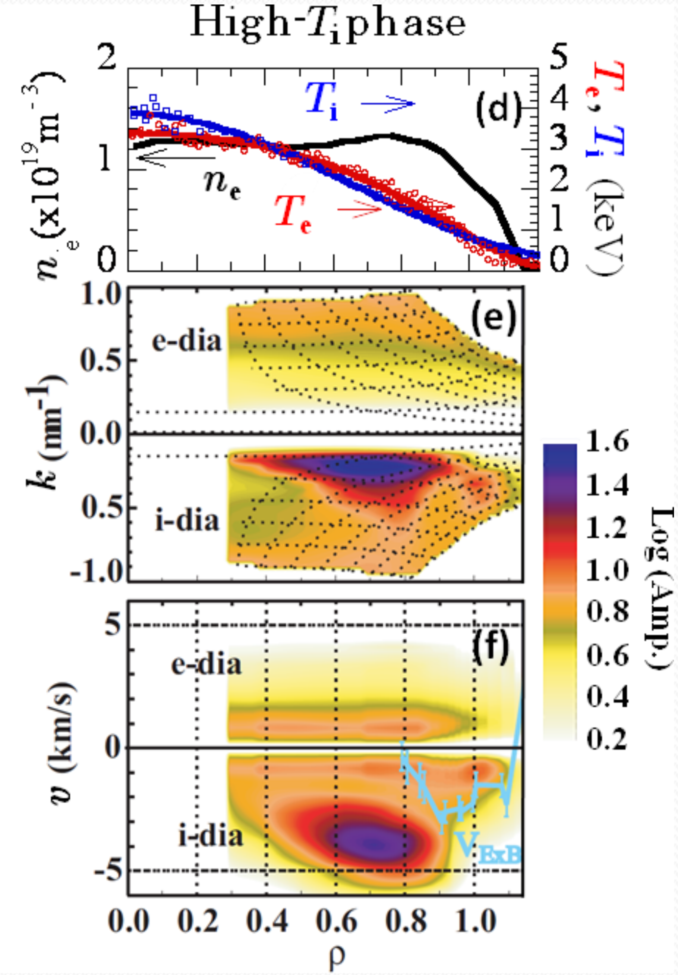

Tanaka et al. PFR 2010

- GKV-X simulations for LHD high-T_i plasma with the 3D experimental configuration.

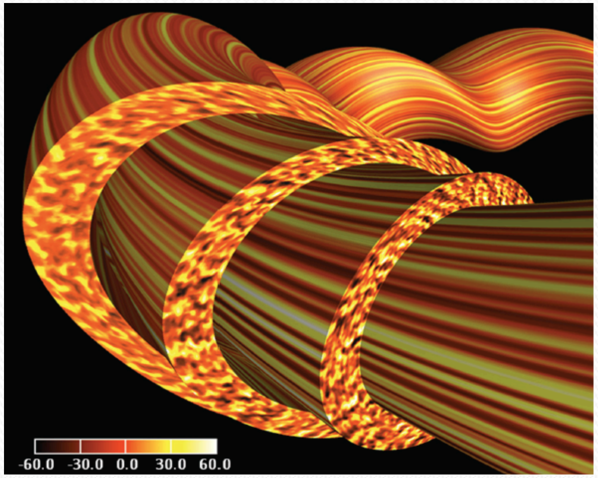

Nunami et al. PoP 2012

- Observed density fluctuations are consistent with results of the ITG turbulence simulations

Transport model developed from GKV simulations

(Nunami *et al.*, PoP **20**, 092307 (2013))

An ITG turbulent transport model is developed:

$$\frac{\chi_i^{\mathrm{model}}}{\chi_i^{\mathrm{GB}}} = \frac{A_1 \left(\sum_k \tilde{\gamma}_k / \tilde{k}_y^2 \right)^{\alpha}}{A_2 + \tilde{\tau}_{\mathrm{ZF}} / \left(\sum_k \tilde{\gamma}_k / \tilde{k}_y^2 \right)^{1/2}}$$

$$\begin{aligned} A_1 &= C_1 C_{\mathcal{T}}^{\alpha+1/2} C_{\mathcal{Z}}^{-1} \\ &= 1.8 \times 10^1 \\ A_2 &= C_2 C_{\mathcal{T}}^{1/2} C_{\mathcal{Z}}^{-1} \\ &= 5.1 \times 10^{-1} \end{aligned}$$

Ion heat diffusivity in high-T_i LHD plasma

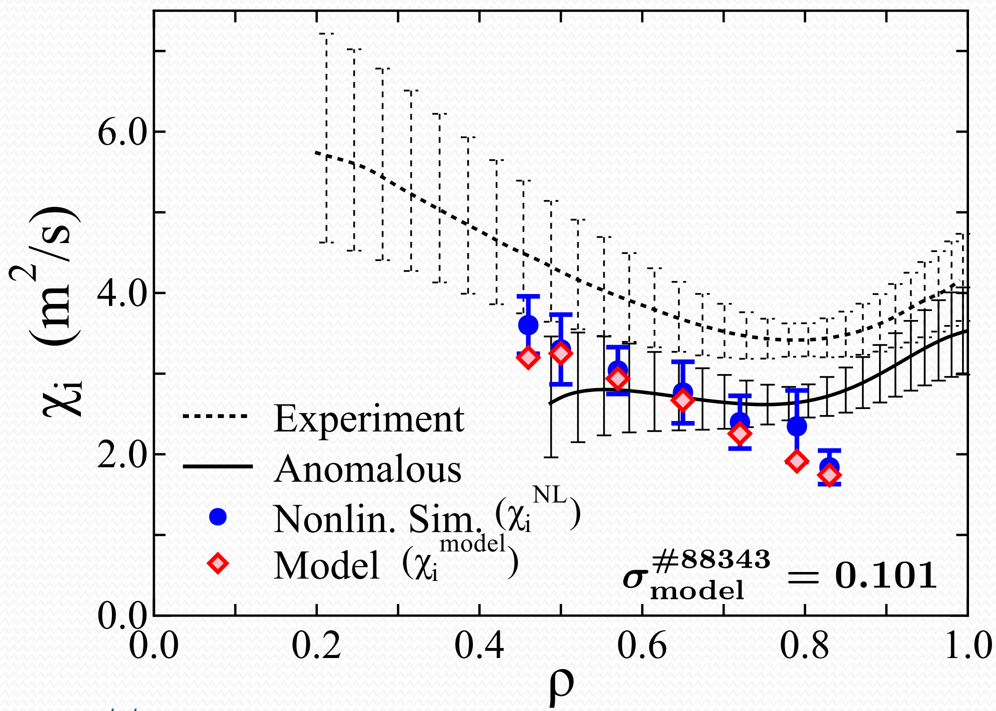

Comparison with nonlinear runs

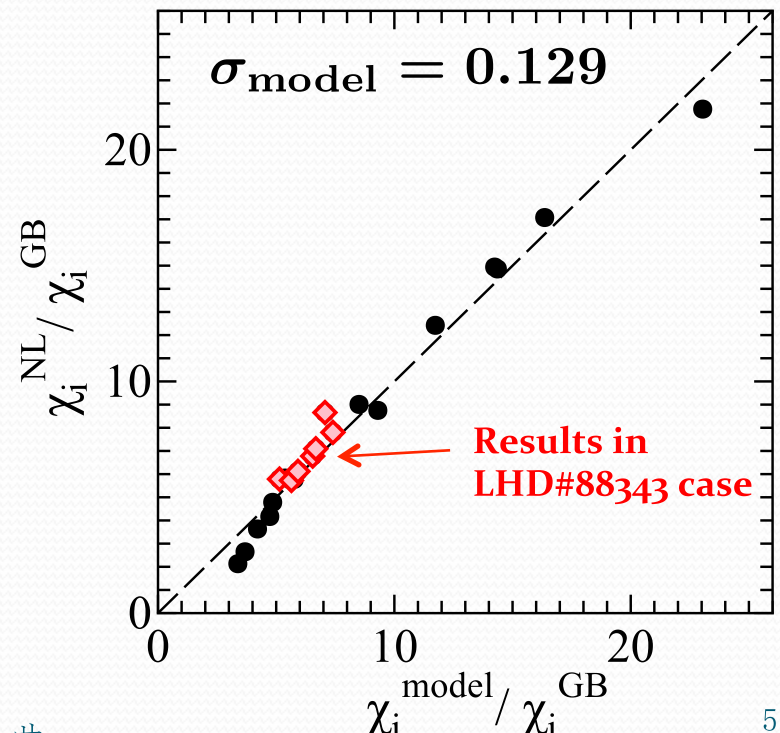

Development of GKV simulations

- Short history of GKV

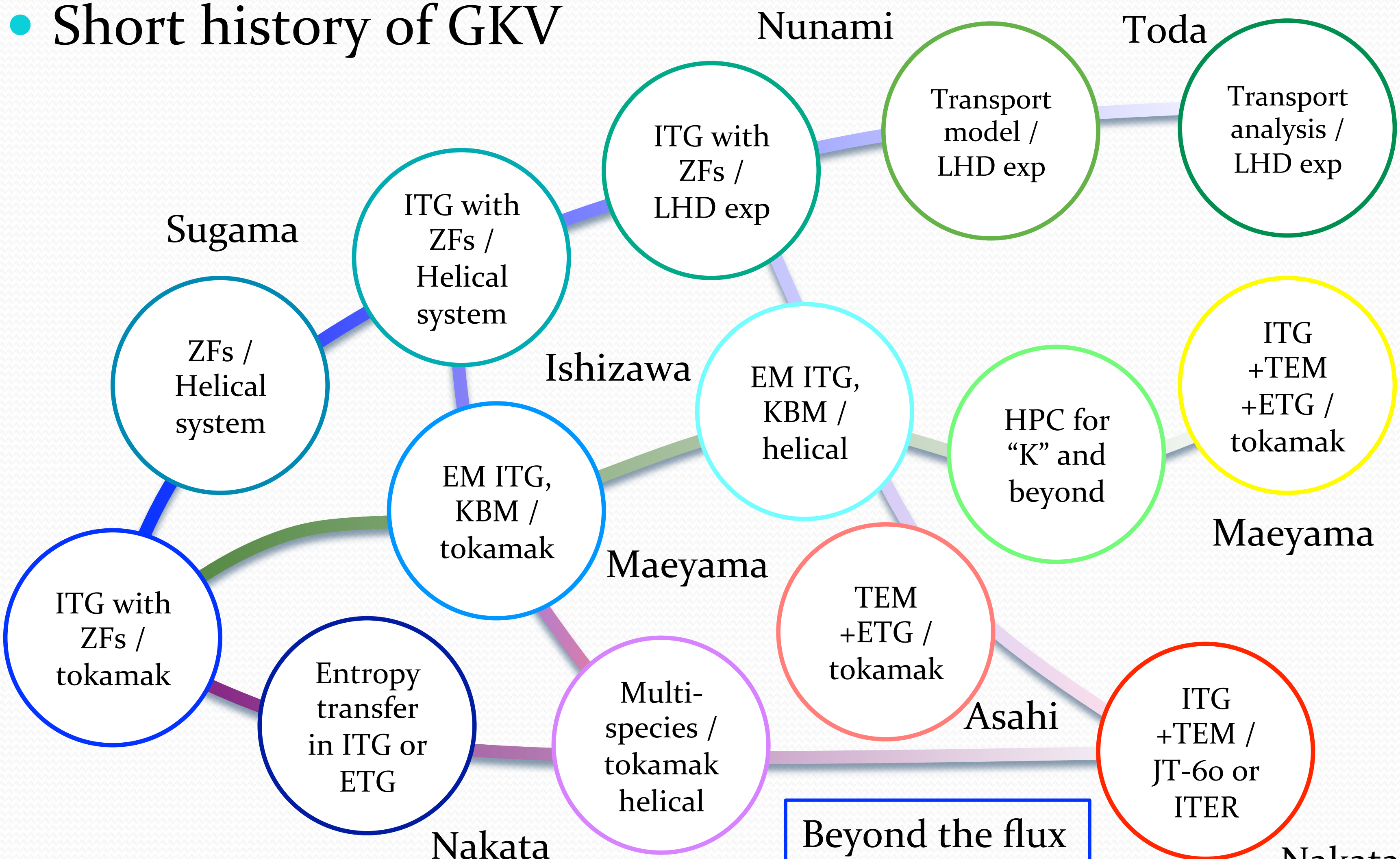

Beyond the flux tube model

Development of GKV simulations

- Short history of GKV

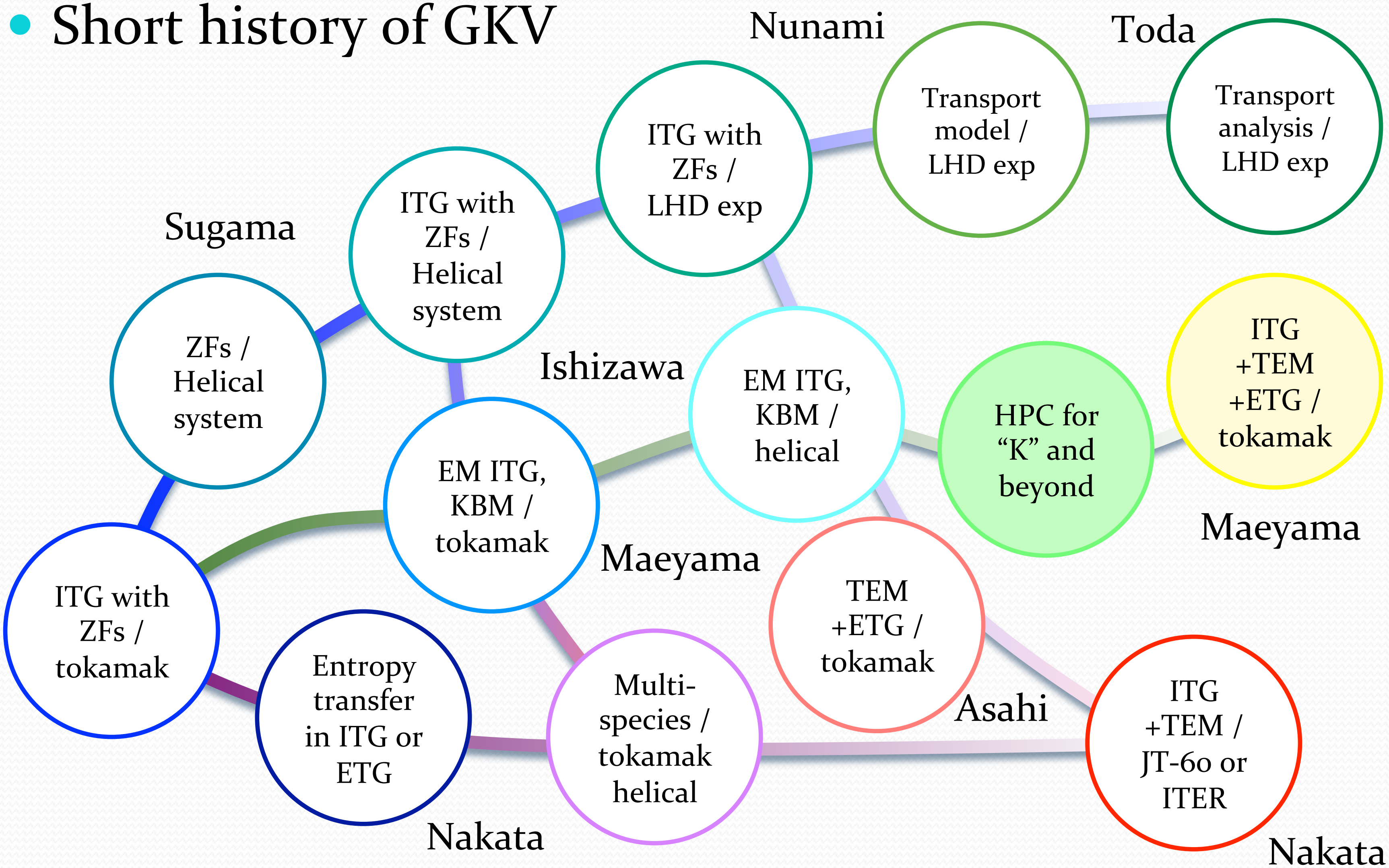

High Performance Computing with GKV

Maeyama et al (2013)

Motivation

- Multi-scale ITG/TEM/ETG turbulence simulations require huge computational costs.

(Grids~10^{11}; Time steps~10^5; Parallelization~100k)

=> Improvement of strong scaling is critically important.

Results

- Multi-dimensional domain decomposition
- Optimized MPI-process mapping (on 3D torus)
- Comput.-commun. Overlap

=> GKV shows excellent strong scaling up to ~600k cores with high parallelization rate 99.99994%.

Strong scalings of GKV

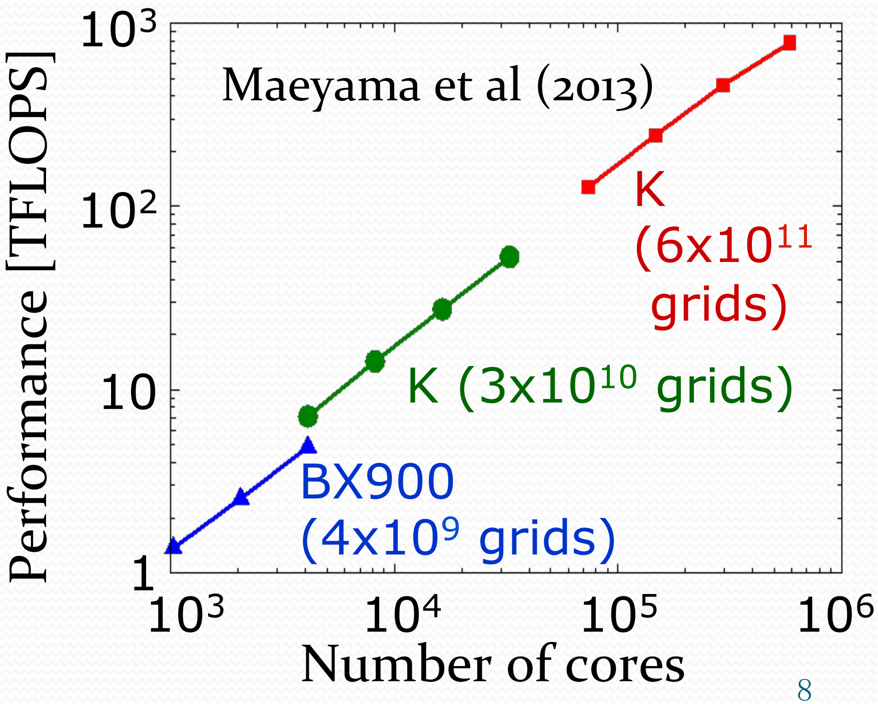

Multi-scale ITG/TEM/ETG turbulence

Results

Maeyama et al (2014)

- ITG turbulence eliminates ETG streamers and dominates heat transport even with real mass ratio.
- When ITGs are weakly unstable (by a finite β effect), the heat transport is enhanced in the multi-scale turbulence, where zonal flows are weakened by electron scale turbulence.

<u>Evolution of electrostatic potentials</u>

(a) At first, ETG driven streamers dominate

(b) Finally, ITGs dominate and ETGs are eliminated.

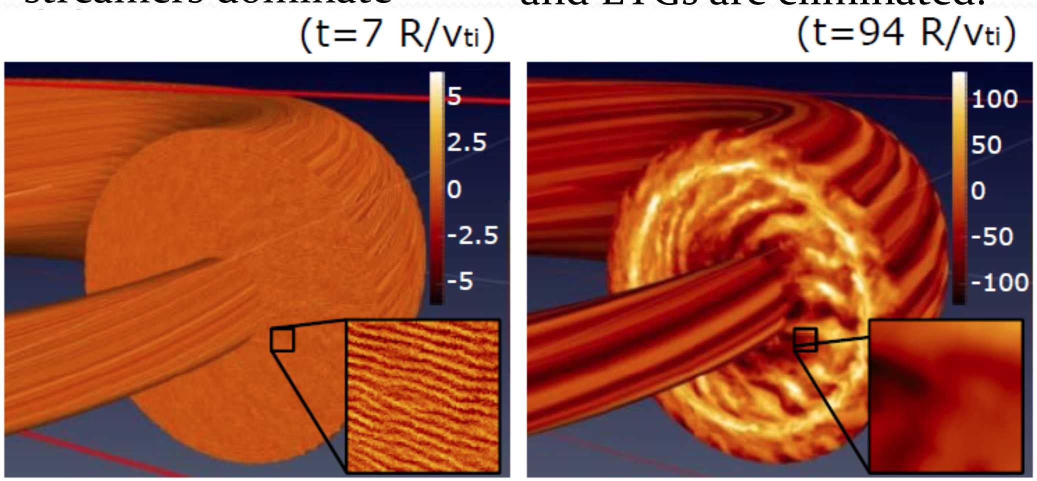

<u>Spectrum of χ_e</u>

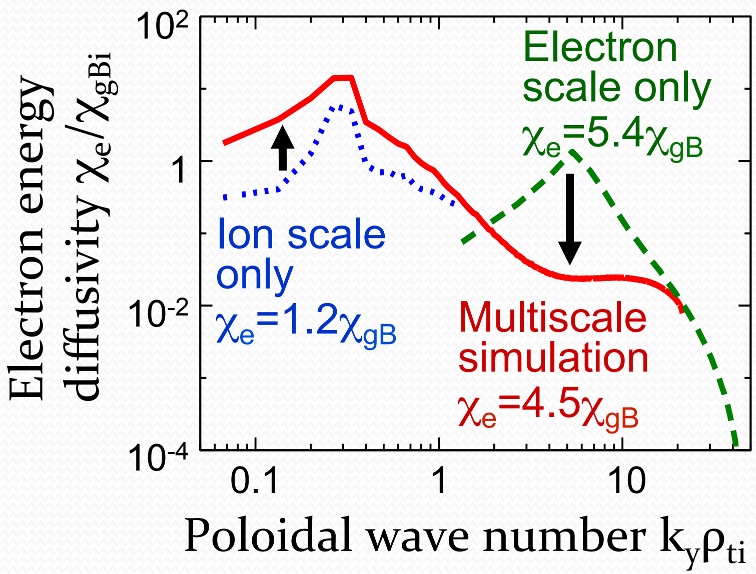

Development of GKV simulations

- Short history of GKV

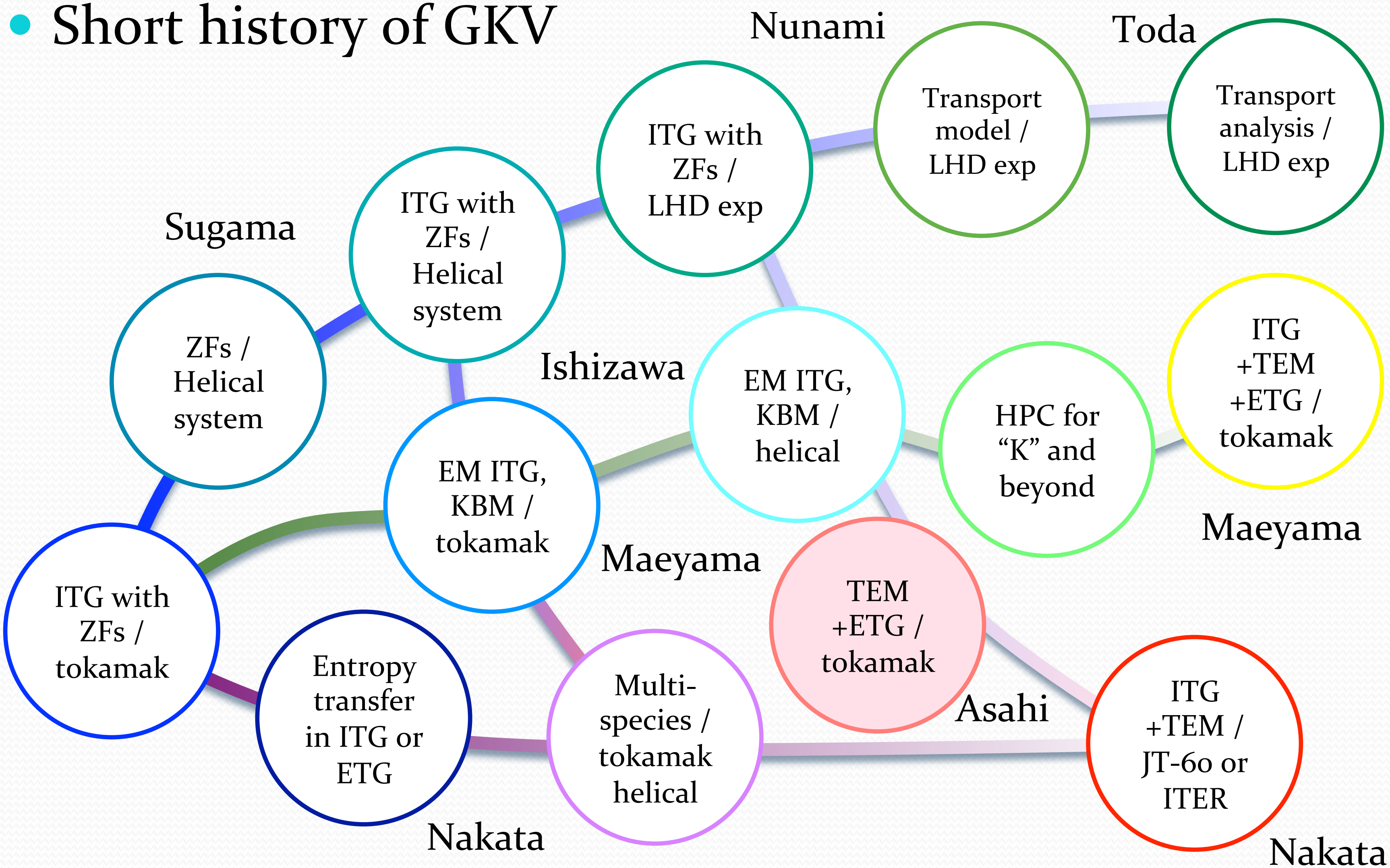

Competition of TEM and ETG turbulence (w/o ITG)

- To investigate the competing process in the multi-scale turbulence, we focus on the electron transport in case w/o ion temperature gradient, where TEM and ETG are unstable.
- Transport reduction is observed in case with kinetic ions after the saturation of the initial ETG mode growths.

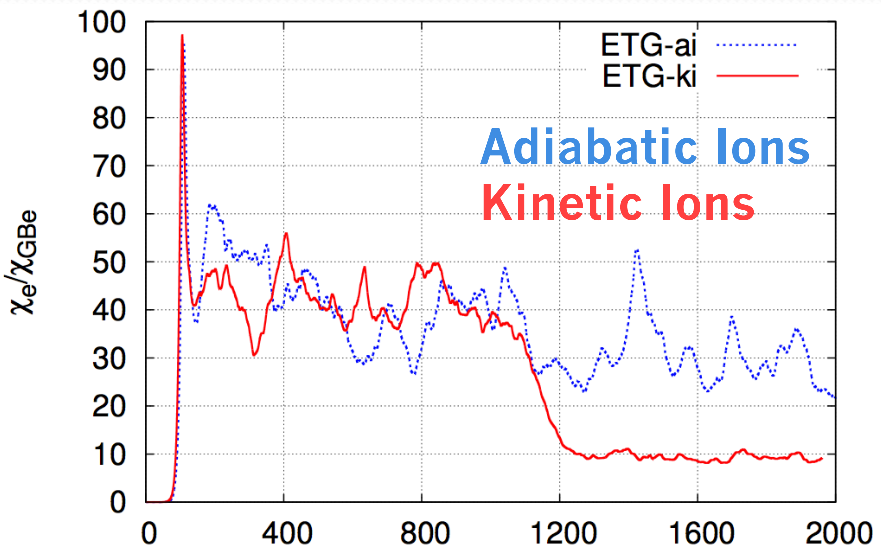

Asahi et al (PoP 2014)

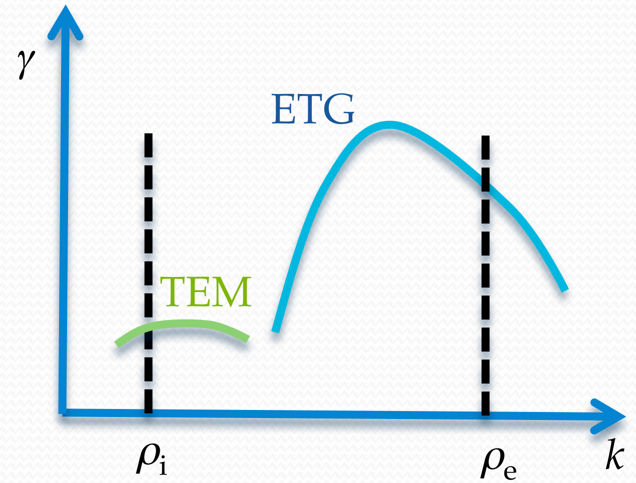

ε = 0.18, s= 0.4, q = 1.4, R_0/L_n=3.46, L_n/L_{Te}=2, L_n/L_{Ti}=0, T_e=T_i, $\nu_e L_n/v_{Te}$= $\nu_i L_n/v_{Ti}$= 0.001

IFERC-CSC

Strong zonal flow suppresses the TEM & ETG turbulence

- Stronger zonal flow generation by TEM leads to the reduction of electron heat transport

Before transition (ETG dominant at t=300)

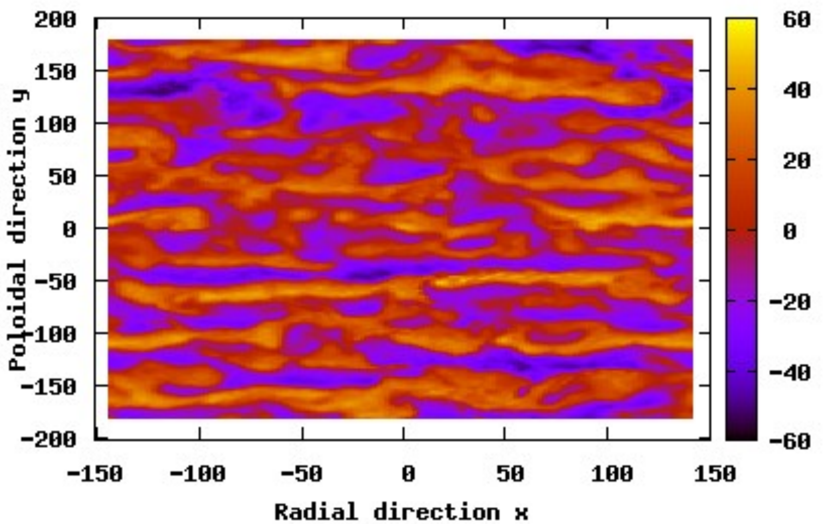

After transition (ZF dominant at t=3500)

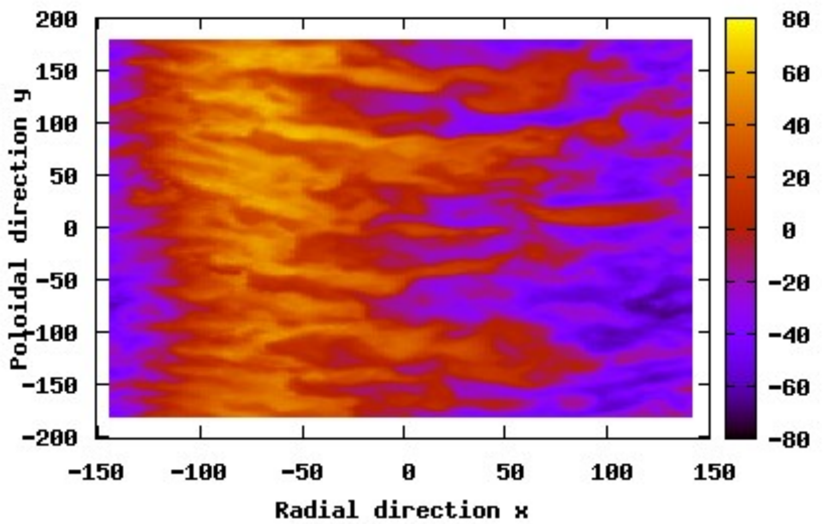

Asahi et al (PoP 2014) (Results from a large-box-size case)

IFERC-CSC

Development of GKV simulations

- Short history of GKV

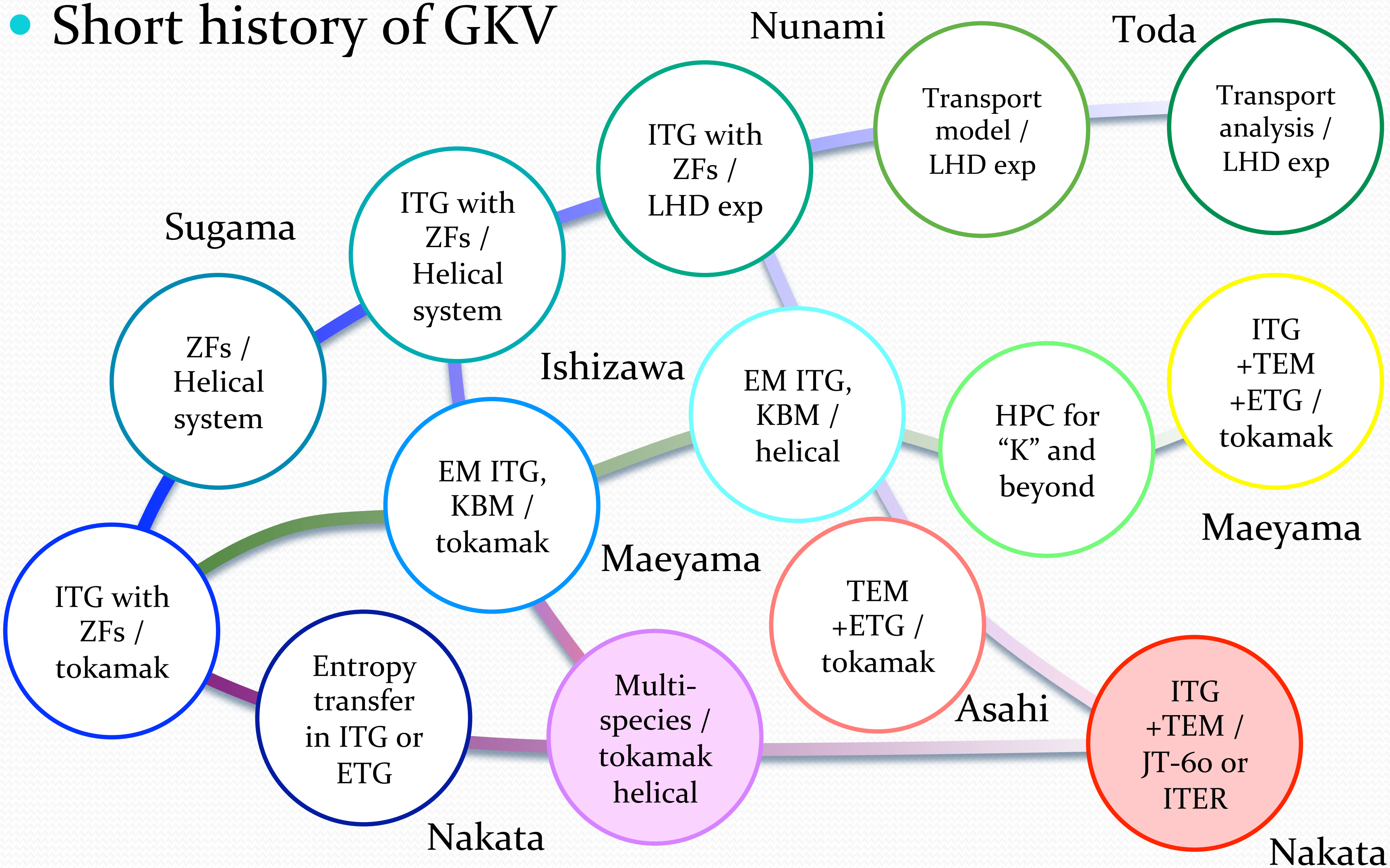

Multi-species turbulence simulation model

M. Nakata and M. Nunami et al, 2014

- **Extension to multi-species(MS) GK model including kinetic electrons and MS-collisions:**

$$\left(\frac{\partial}{\partial t} + v_\parallel \boldsymbol{b}\cdot\nabla + i\omega_{\mathrm{Da}}\right)\delta h_{\mathrm{a}\boldsymbol{k}_\perp} - \frac{c}{B}\sum_{\Delta} \boldsymbol{b}\cdot(\boldsymbol{k}'_\perp \times \boldsymbol{k}''_\perp)\,\delta\psi_{\mathrm{a}\boldsymbol{k}'_\perp}\,\delta h_{\mathrm{a}\boldsymbol{k}''_\perp} = \frac{e_{\mathrm{a}} F_{\mathrm{Ma}}}{T_{\mathrm{a}}}\left(\frac{\partial}{\partial t} + i\omega_{*T\mathrm{a}}\right)\delta\psi_{\mathrm{a}\boldsymbol{k}_\perp} + C_{\mathrm{a}}^{(\mathrm{GK})}(\delta h_{\mathrm{a}\boldsymbol{k}_\perp})$$

$$C_{\mathrm{a}}^{(\mathrm{GK})} = \sum_{\mathrm{b}} C_{\mathrm{ab}}^{(\mathrm{GK})}[\delta h_{\mathrm{ak}_\perp}, \delta h_{\mathrm{bk}_\perp}] \equiv \sum_{\mathrm{b}} \oint \frac{d\varphi}{2\pi} e^{i\boldsymbol{k}_\perp\cdot\boldsymbol{\rho}_{\mathrm{a}}} \left\{ C_{\mathrm{ab}}^{\mathrm{TS}}[e^{-i\boldsymbol{k}_\perp\cdot\boldsymbol{\rho}_{\mathrm{a}}}\delta h_{\mathrm{ak}_\perp}] + C_{\mathrm{ab}}^{\mathrm{F}}[e^{-i\boldsymbol{k}_\perp\cdot\boldsymbol{\rho}_{\mathrm{b}}}\delta h_{\mathrm{bk}_\perp}] \right\}$$

Sugama et al, PoP2009

- **Test-particle operator for arbitrary multiple particle species**

$$C_{\mathrm{ab}}^{TS} = C_{\mathrm{ab}}^{T0} + (\theta_{\mathrm{ab}} - 1)\left(\mathcal{P}_{\mathrm{a}} C_{\mathrm{ab}}^{T0} + C_{\mathrm{ab}}^{T0}\mathcal{P}_{\mathrm{a}}\right) + (\theta_{\mathrm{ab}} - 1)^2 \mathcal{P}_{\mathrm{a}} C_{\mathrm{ab}}^{T0} \mathcal{P}_{\mathrm{a}}$$

$C_{\mathrm{ab}}^{T0} = \nu_{\mathrm{D}}^{\mathrm{ab}}\mathcal{L} + C_v^{\mathrm{ab}}$: pitch-angle scattering and energy diffusion

Note: Conventional operators [e.g., Abel PoP2008, Barnes PoP2009] can be applied only for isothermal (T_a=T_b) species, and the energy conservation for ion-electron are ignored.

- **Improved field-particle operator ensuring conservation properties**

$$\hat{C}_{\mathrm{ab}}^{F} = -\frac{\overline{\sigma_{\mathrm{ab}}(v)}}{\left\langle \overline{\sigma_{\mathrm{ab}}(v)} \right\rangle}\hat{N}_{\mathrm{ab}} - \frac{C_{\mathrm{ab}}^{TS}(F_{\mathrm{Ma}} m_{\mathrm{a}} v_\parallel / T_{\mathrm{a}})}{\left\langle m_{\mathrm{a}} v_\parallel C_{\mathrm{ab}}^{TS}(F_{\mathrm{Ma}} m_{\mathrm{a}} v_\parallel / T_{\mathrm{a}}) \right\rangle}\hat{V}_{\mathrm{ba}} - \frac{\overline{C_{\mathrm{ab}}^{TS}(F_{\mathrm{Ma}} x_{\mathrm{a}}^2)}}{\left\langle (m_{\mathrm{a}} v^2/2)\overline{C_{\mathrm{ab}}^{TS}(F_{\mathrm{Ma}} x_{\mathrm{a}}^2)} \right\rangle}\hat{E}_{\mathrm{ba}}$$

Nakata & Nunami et al, 2014

---> Particle/momentum/energy-conservations are accurately satisfied within $O(10^{-16})$.

Benchmark test of thermal equilibration

Nunami et al. 18PB-115

Test of thermal equilibration processes in three-ion species case with deuterium, helium and carbon. If each species ion has the perturbed Maxwellian distributions with different temperature,

$$\delta f_a = F_{a\mathrm{M}}\left(\frac{\delta n_a}{n_a} + \left(\frac{m_a}{T_a}\right)\vec{u}_a\cdot\vec{v} + \frac{\delta T_a}{T_a}\left(\frac{v^2}{v_{\mathrm{t}a}^2} - \frac{3}{2}\right)\right)$$

thermal equilibration of *a*-species ions is given by

$$\frac{\partial}{\partial t}\delta f_a = \sum_b \left(C_{ab}^{\mathrm{T}}(\delta f_a) + C_{ba}^{\mathrm{F}}(\delta f_b)\right)$$

Time evolutions of the temperature fluctuations dT_a/T_a

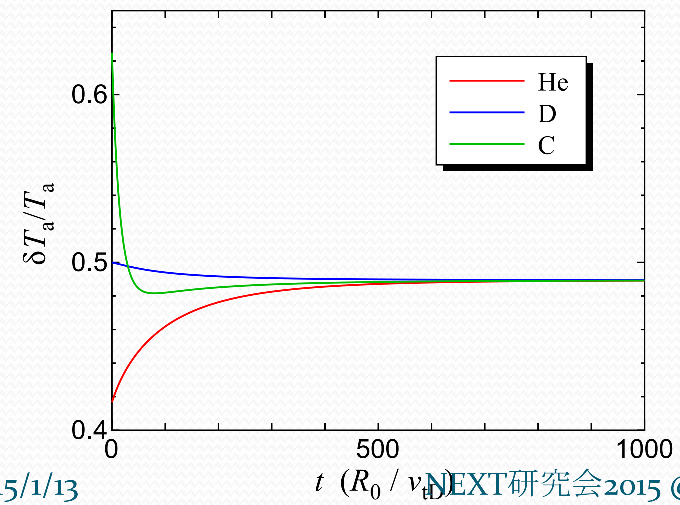

Distribution functions at t=0 & t=1000 [R_0/v_{tD}]

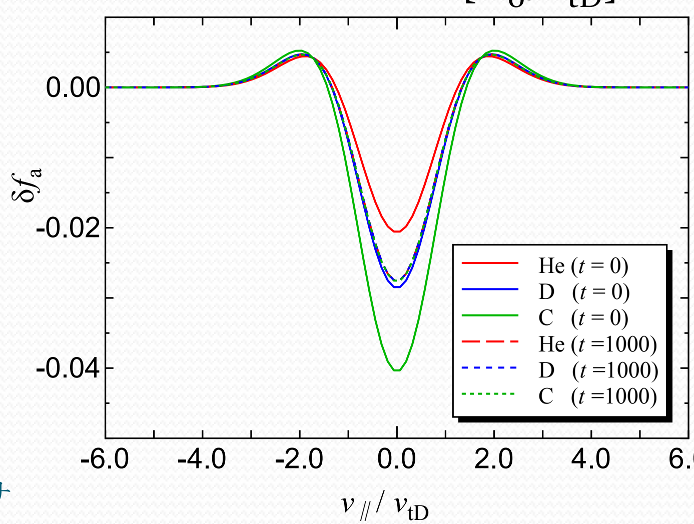

Beyond the conventional flux tube model

Turbulence correlation may widely expand along field lines

Linear eigenfunction of ITG/ETG for the Cyclone case with weak shear ($\hat{s} = 0.2$)

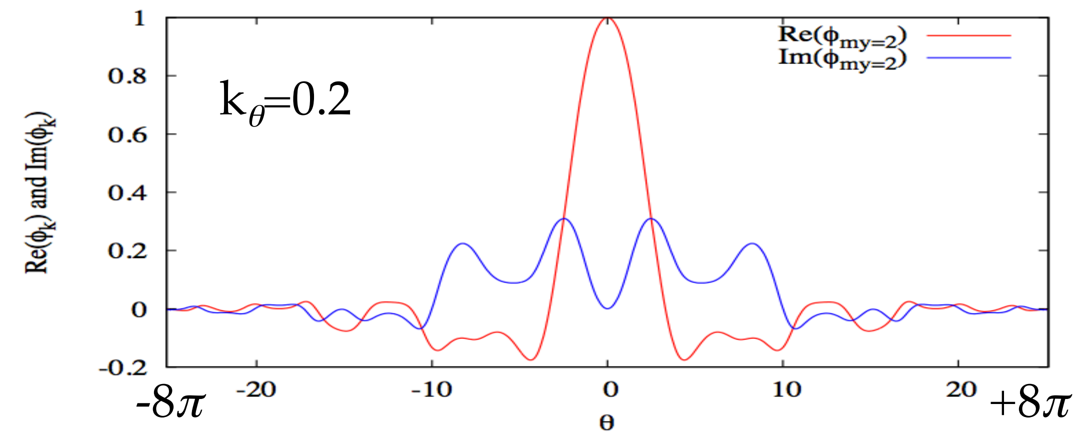

Parallel correlation of the ITG turbulence for the Cyclone case with $\hat{s} = 0.2$

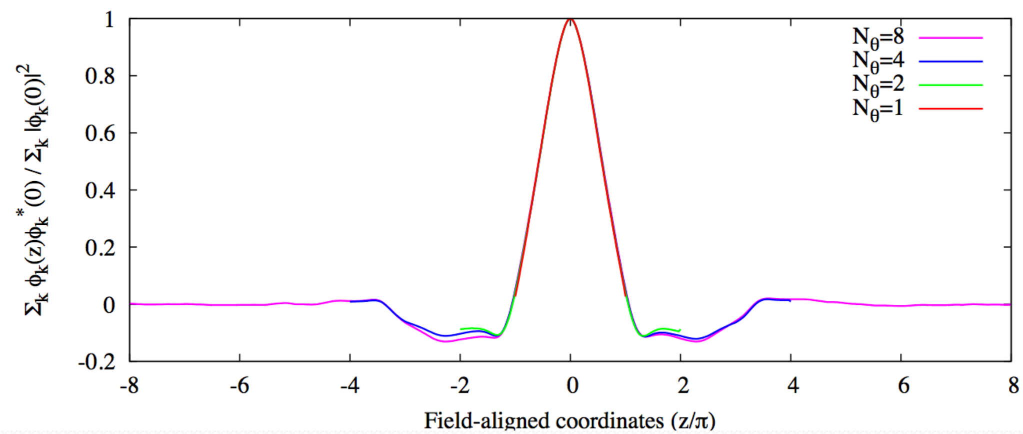

- Turbulent interactions at $|\theta| > \pi$ may play non-negligible roles
- Larger N_θ => severer Courant condition & symmetry breaking

Symmetry in δf GK equations

$$\left(\frac{\partial}{\partial t} + v_\parallel \boldsymbol{b}\cdot\nabla + i\omega_{Ds} - \frac{\mu}{m_s}\boldsymbol{b}\cdot\nabla B \frac{\partial}{\partial v_\parallel}\right) h_{s,\boldsymbol{k}_\perp} - \sum_{\boldsymbol{k}_\perp = \boldsymbol{k}'_\perp + \boldsymbol{k}''_\perp} \boldsymbol{b}\cdot\boldsymbol{k}'_\perp \times \boldsymbol{k}''_\perp \psi_{\boldsymbol{k}'_\perp} h_{s,\boldsymbol{k}''_\perp}$$
$$= F_{Ms}\left(\frac{\partial}{\partial t} + i\omega_{*Ts}\right)\frac{e_s\psi_{\boldsymbol{k}_\perp}}{T_s} + C_s(h_{s,\boldsymbol{k}_\perp}) \ ,$$

$$\boldsymbol{k}_\perp = k_x\nabla x + k_y \nabla y$$
$$= c_x(k_x + c_\theta \hat{s}\theta k_y)\nabla\rho + c_y k_y (q_0\nabla\theta - \nabla\zeta)$$

$$h_{s,\boldsymbol{k}_\perp} = \delta f^{(g)}_{s,\boldsymbol{k}_\perp} + J_{0s}\frac{e_s\phi_{\boldsymbol{k}_\perp}}{T_s}F_{Ms} \ ,$$

$$\omega_{Ds} = \frac{m_s v_\parallel^2 + \mu B}{m_s\Omega_s B^2\sqrt{g_{\rho\theta\zeta}}}\left[c_x(k_x + c_\theta\hat{s}\theta k_y)\left(B_\theta\frac{\partial B}{\partial\zeta} - B_\zeta\frac{\partial B}{\partial\theta}\right)\right.$$
$$\left. + c_y q_0 k_y\left(B_\zeta\frac{\partial B}{\partial\rho} - B_\rho\frac{\partial B}{\partial\zeta}\right) - c_y k_y\left(B_\rho\frac{\partial B}{\partial\theta} - B_\theta\frac{\partial B}{\partial\rho}\right)\right]$$

Symmetry $\theta \to \theta + 2\pi p$ and $k_x \to k_x - 2\pi p c_\theta \hat{s} k_y$

The ExB NL term also preserves the symmetry

$$(\boldsymbol{k}'_\perp + \delta\boldsymbol{k}'_\perp)\times(\boldsymbol{k}''_\perp + \delta\boldsymbol{k}''_\perp) = \boldsymbol{k}'_\perp \times \boldsymbol{k}''_\perp \ , \quad \text{for } \delta\boldsymbol{k}'_\perp = c_\delta k'_y \nabla x \text{ and } \delta\boldsymbol{k}''_\perp = c_\delta k''_y\nabla x$$

Turbulent fluctuations in flux tube simulations

$$\theta \to \theta + 2\pi p \text{ and } k_x \to k_x - 2\pi p c_\theta \hat{s} k_y$$

Symmetry in GK equation

- Conventional Model

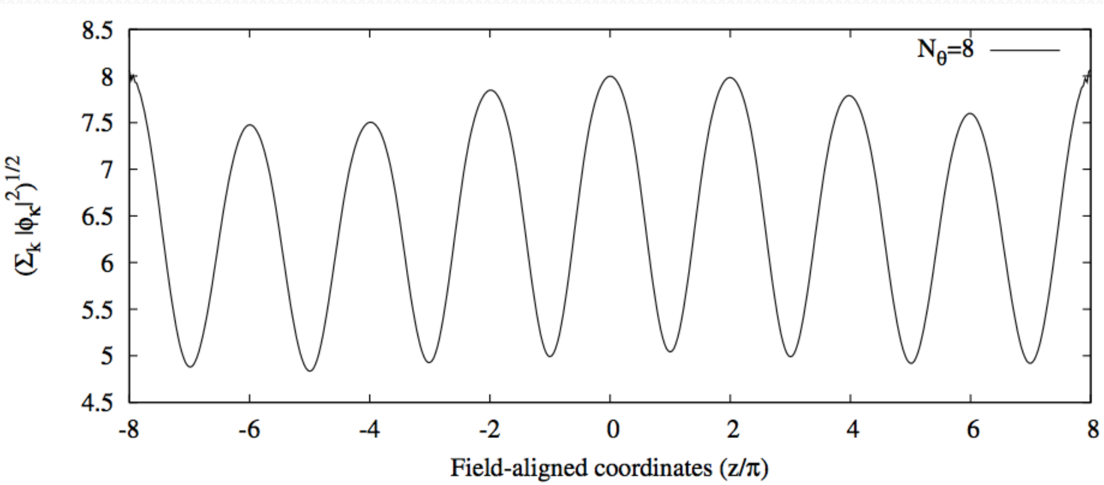

- Flux tube train model

New Method !

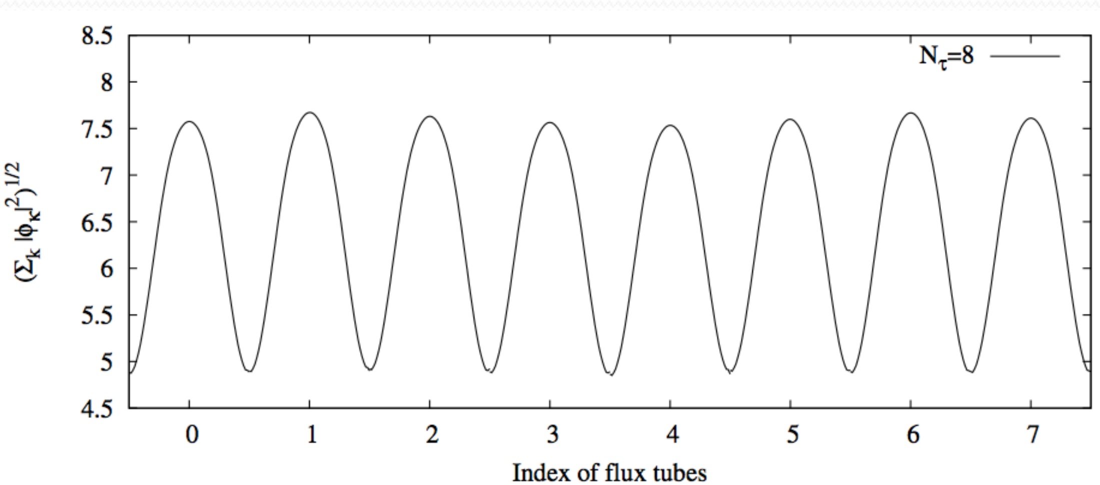

"Flux tube train" model

- A new model with a train of flux tubes serially connected with the boundary condition of

$$A[\psi,\alpha(\theta+2\pi,\varsigma),z(\theta+2\pi)]_l = A[\psi,\alpha(\theta,\varsigma),z(\theta)]_{l+1}$$

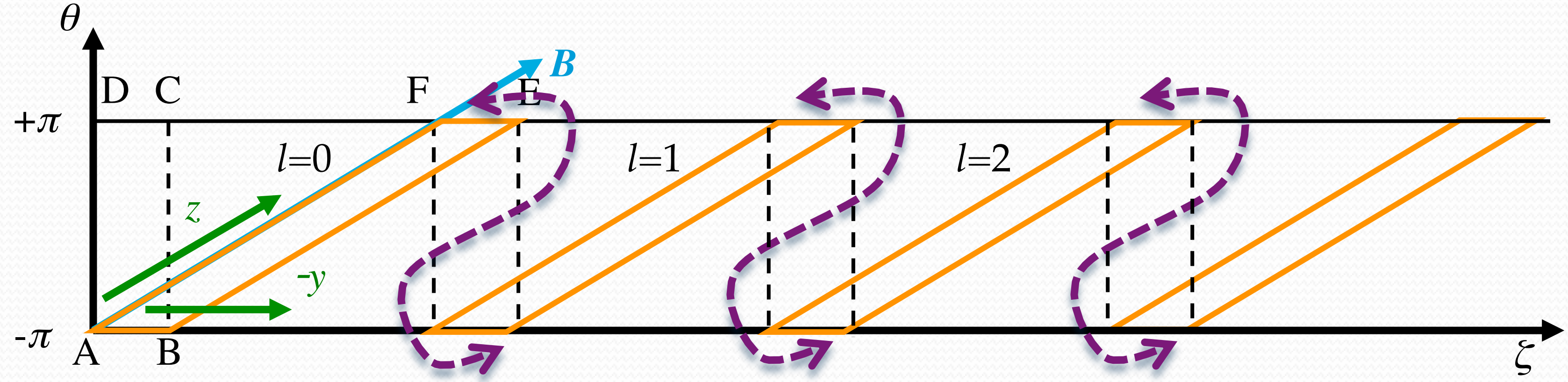

  - Flux tube of $l=N_t$-1, is connected to that of l=0
  - Relation to conventional flux tube; $\theta_l = \theta - 2\pi l$
  - Turbulence simulation is carried out in *each* flux tube
- Equivalent to the conventional flux tube model in the continuum limit but free from the secular increase of k_x to θ.

Similarity to the ballooning representation

- Ballooning representation

$$A_n(\psi,\theta) = \sum_{p=-\infty}^{\infty} \hat{A}_{n,\theta_0}(\psi,\theta+2\pi p)\exp\left[-inq(\psi)(\underline{\theta-\theta_0+2\pi p})\right]$$

- Conventional flux tube model with the period of $2N_\theta\pi$

$$A_n(\psi,\theta) = \sum_{j=-\infty}^{\infty} \bar{A}_{j,n}(\theta)\exp\left\{-inq(\psi)[\theta-\theta_0(j,n)]\right\}$$
$$= \sum_{j=0}^{\delta j-1}\sum_{p=-\infty}^{\infty} \bar{A}_{j,n}(\theta+2\pi pN_\theta)\exp\left\{-inq(\psi)[\theta-\underline{\theta_0(j,n)+2\pi pN_\theta}]\right\}$$

- Flux tube train model with l = 0, 1, 2, …, N_t

$$A_n(\psi,\theta) = \sum_{j=-\infty}^{\infty} \bar{A}_{j+l\delta j/N_t,n}(\theta)\exp\left\{-inq(\psi)[\theta-\theta_0(j+l\delta j/N_t,n)]\right\}$$
$$= \sum_{j=-\infty}^{\infty} \bar{A}^{l}_{j,n}(\theta-2\pi l)\exp\left\{-inq(\psi)[\theta-\underline{\theta_0(j,n)-2\pi l}]\right\}$$

$$n\theta_0 = j\pi/\Delta q$$
$$j\pi = k_x r_0 \Delta q/q_0\hat{s}$$
$$n = -k_y r_0/q_0$$

Turbulent fluctuations in flux tube simulations

$$\theta \to \theta + 2\pi p \text{ and } k_x \to k_x - 2\pi p c_\theta \hat{s} k_y$$

Symmetry in GK equation

- Conventional Model

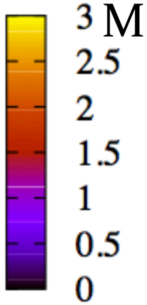

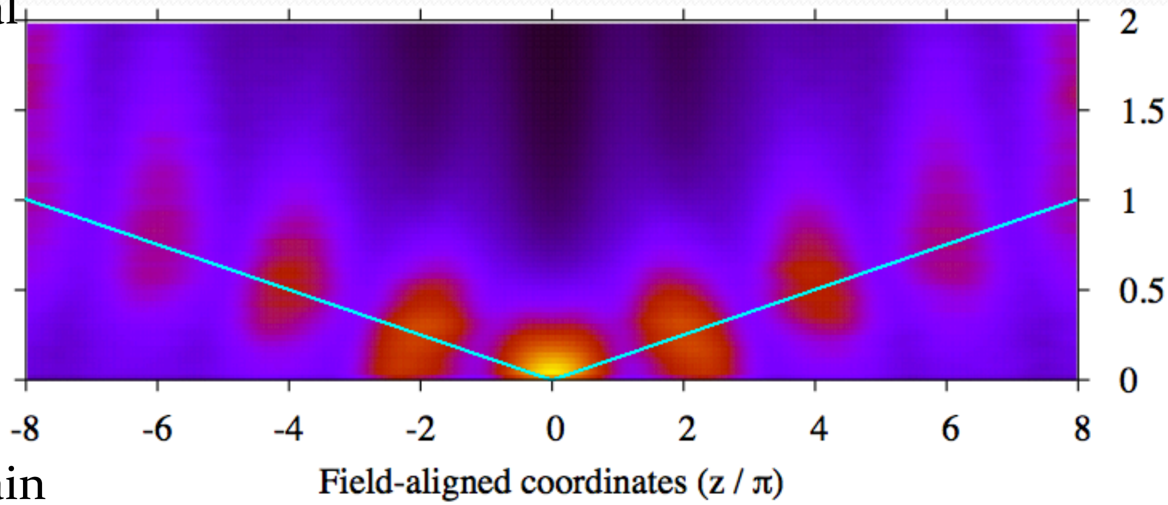

Solid Line

$k_x = | \hat{s} z k_y |$

$\hat{s} = 0.2, k_y = 0.2$

- Flux tube train model

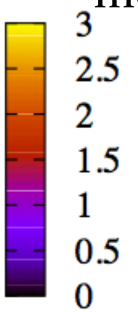

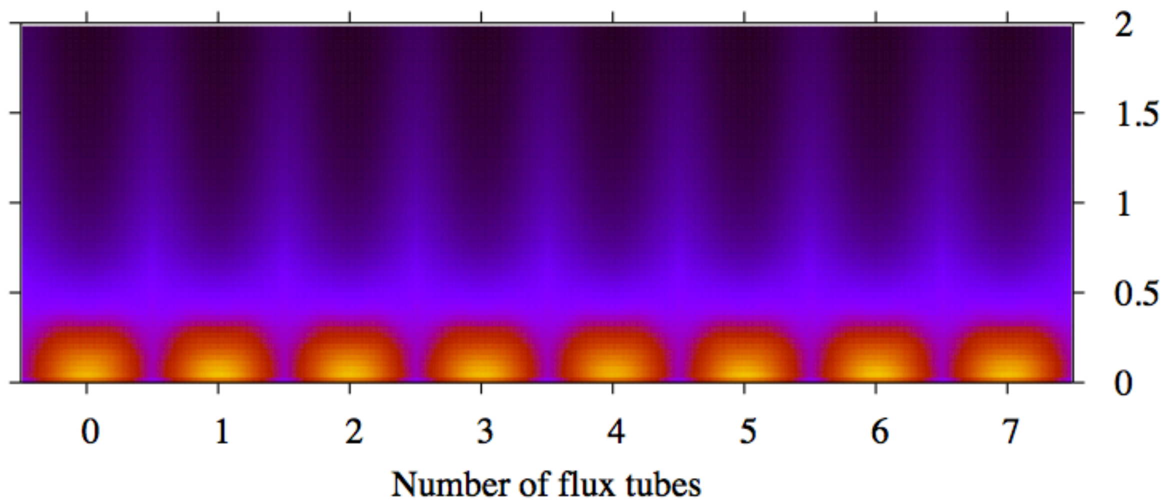

Comparison of ion heat transport

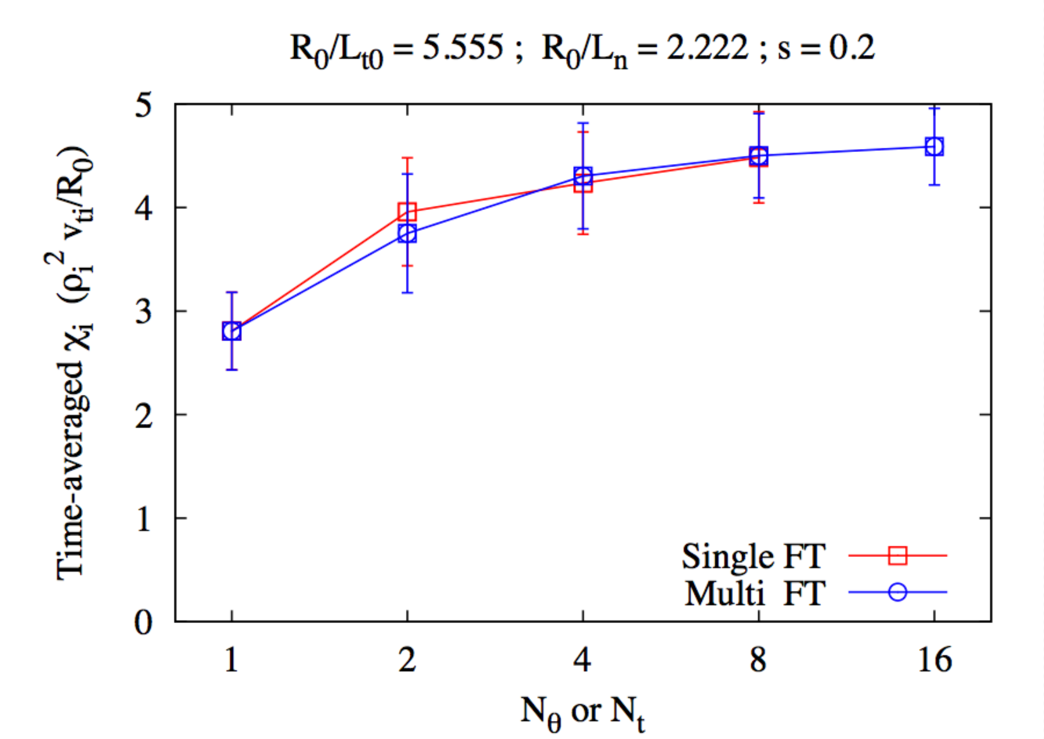

$k_{y,\min}\,\rho_i$=0.05

- Results of "flux tube train" model agree with those of a single flux tube for N_θ=N_t =< 8. However, the conventional model has the severer CLF condition as $k_\perp^2 = (k_x + \hat{s}\theta k_y)^2 + k_y^2$ and was numerically unstable for N_θ> 8.

Future directions

- Further applications and extensions of the GKV code will be carried out for more reliable prediction of turbulent transport in magnetically confined fusion plasmas towards ITER and beyond!
  - Multi-species simulations
  - Introduction of a mean flow to local turbulence model
  - Momentum transport
- Comprehension of magnetized plasma turbulence
  - Phase space turbulence in 5-D
    - Energy (entropy) input, cascading, and dissipation processes
  - Application to space and astrophysical conditions
    - Stellar wind turbulence, magnetic reconnection, etc.